Journal of Solid State Chemistry **147,** 211–217 (1999)
Article ID jssc.1999.8226, available online at http://www.idealibrary.com on IDEAL®

Interplay between Local Electronic Configuration and the Occurrence of a Metallic State: An Experimental Approach

Jean-Pierre Doumerc,[1] Jean-Claude Grenier, Paul Hagenmuller, Michel Pouchard, and Antoine Villesuzanne

ICMCB-CNRS, Château Brivazac, 87, avenue du Dr. A. Schweitzer, 33608 Pessac, France

Received November 4, 1998; in revised form February 5, 1999; accepted February 15, 1999

DEDICATED TO THE MEMORY OF JEAN ROUXEL

Assuming that structural distortions are involved in a large class of metal–insulator transitions as well as in the stabilization of the local electronic configuration of a given cation leads the authors to look for a chemical system appropriate for investigating the interplay between both effects. The chosen cobaltite, $TlSr_2CoO_5$, undergoes a first order phase transition near room temperature involving steep changes and a hysteresis loop in the temperature dependencies of the magnetic susceptibility and of the electrical resistivity. The low temperature o-phase is an antiferromagnetic semiconductor and the high temperature *t*-phase is a metal with dominant ferromagnetic interactions. Electronic structure was calculated using the extended Hückel tight-binding method. The metallic character of the *t*-phase can be explained by the delocalization of some of the *d*-electrons of Co^{3+}-ions in a $\sigma^*_{x^2-y^2}$ band and the strong ferromagnetic interactions can be ascribed to an indirect coupling of the localized moments *via* itinerant electrons. The electronic configuration of cobalt ions can be regarded as intermediate between high-spin and intermediate-spin states in the *t*-phase. In the low temperature phase it disproportionates into a purely high-spin state and a purely intermediate-spin state for Co^{3+} ions located in two different sites, the features of which respectively accommodate each electronic configuration.

1. INTRODUCTION

Electronic states in solids can be described either in terms of localized orbitals (e.g., atomic orbitals) or in terms of extended states (e.g., Bloch functions). Generally the first type of description is appropriate for the interpretation of electronic properties of insulators such as magnetic properties. The second one is more pertinent for explaining electronic transport involving band-type conduction like in metals or semiconductors and hence for describing a number of metal–insulator (MI) transitions. In this paper we mainly deal with MI transitions monitored by a temperature change. Among them can be found MI transitions where a metallic-type state is associated with the occurrence of a ferromagnetic long range ordering like in the well-known manganites exhibiting giant magnetoresistance. In this case the metallic-type state is observed at low temperature as carrier scattering by the local spins (due to t_{2g} electrons of Mn ions) is reduced by the long range ordering, whereas in the other cases it occurs above the transition temperature (T_{MI}), the system being insulating at 0 K.

Most of the temperature dependent MI transitions involve a rather distorted phase at low temperatures and a more symmetric one above T_{MI}. Actually the distorted phase is stable at 0 K as it corresponds to the lowest energy of the electronic system. In other words the gain in electronic energy overcomes the loss of elastic energy required to distort the crystal structure. The insulating character of the low temperature (LT) phase results from the splitting of the conduction band by the translational symmetry, the specimen of such transitions being the well-known Peierls transition.

On the other hand, the local electronic configuration and spin state depend on the strength of the crystal field and on the site distortion. The purpose of the present paper is to discuss on the basis of recent experimental data and extended Hückel tight-binding (EHTB) calculations the interplay between the local electronic configuration involving mainly atomic orbitals and the occurrence of a metalic state involving collective electronic levels.

2. CHOOSING THE CHEMICAL SYSTEM

In some respects, our aim is to investigate how a change in the local electronic configuration, via atomic displacements, could lead to a MI transition. For that purpose we have looked for a cation that can exhibit various electronic

[1]To whom correspondence should be addressed.

0022-4596/99 $30.00

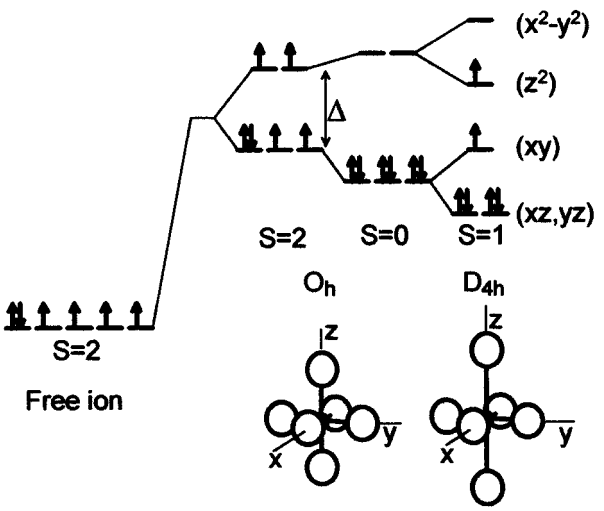

FIG. 1. Possible electronic configurations of Co^{3+} ions.

configurations and for which a strong electron–phonon coupling is expected. Cobalt III seemed a promising choice as, for instance, when it is surrounded by six oxygen atoms, it may exhibit three different spin states depending on the site symmetry (1).

The Co^{3+} ions has six electrons in the 3*d* shell. In the free ion the five 3*d* orbitals are degenerate. According to Hund's rule the ground state of the free ion has a $S = 2$ spin value corresponding to the high spin (HS) configuration (Fig. 1). If the six oxygen atoms are located at the corner of a regular octahedron (O_h symmetry) the *d* orbitals oriented toward the ligands are less stable and provided that the stabilization energy arising from the crystal field parameter, Dq, remains smaller than the variation of the exchange energy, the electronic configuration is $t_{2g}^4 e_g^2$ and the HS state is preserved. For large enough values of Dq, a $t_{2g}^6 e_g^0$ configuration can become the ground state and a low spin (LS) ($S = 0$) state is observed.

When the octahedron is elongated, e.g., along the *z*-axis, an intermediate spin (IS) ($S = 1$) configuration can be stabilized (Fig. 1).

In order to induce such an axial distortion we chose a simple layer structure, that of the 1201 thallium cuprate, $TlSr_2CuO_5$. This structure contains perovskite-type $(Sr_2CuO_4)^-$ slabs linked by Tl atoms located in $(TlO)^+$ layers (Fig. 2). The large anisotropy of the structure favors a strong elongation of the oxygen octahedra surrounding the 3*d*-transition element. Such a feature can hardly occur in a real perovskite compound where the site distortion, if any, is small and rather dynamic as, for instance, in $LaCoO_3$ where the fluctuations of the Co–O distances do not seem to lead to a well-established long range ordering (2). In the 1201 structure, the occurrence of two long axial Co–O distances is enhanced by the existence of strongly covalent axial Tl–O bonds.

Another reason for the choice of this structure is a possible contribution to the understanding of high T_C superconductors owing to the structural analogy and the expectation of strong electron–phonon interactions with Co^{3+}.

3. SAMPLE PREPARATION AND CHARACTERIZATION

Preparation and chemical analysis of $TlSr_2CoO_5$ were described elsewhere (3). The investigated sample is slightly thallium deficient, which results in an average oxidation state of cobalt higher than 3, actually of about 3.05.

$TlSr_2CoO_5$ undergoes a first-order phase transition near room temperature characterized by steep changes in the temperature dependence of the magnetic susceptibility and of the electrical resistivity and by a hysteresis loop (4) (Fig. 3).

The high temperature (HT) form (or *t*-phase) has a tetragonal unit cell that can be described with a *P*4/*mmm* space group already reported for the cuprate analogues. As expected, Co^{3+} ions occupy elongated octahedra with four equatorial short distances and two axial long distances (Fig. 4).

The LT form was first described with a unit cell similar to that of the *t*-phase, but with a significantly larger cell volume. An electron diffraction study showed that the actual unit cell is rather orthorhombic with lattice parameters related to that of the tetragonal cell by the following equation (5):

$$(a_o\ b_o\ c_o) = (a_t\ b_t\ c_t)\begin{pmatrix} 1 & 3 & 0 \\ -1 & 3 & 0 \\ 0 & 0 & 2 \end{pmatrix}.$$

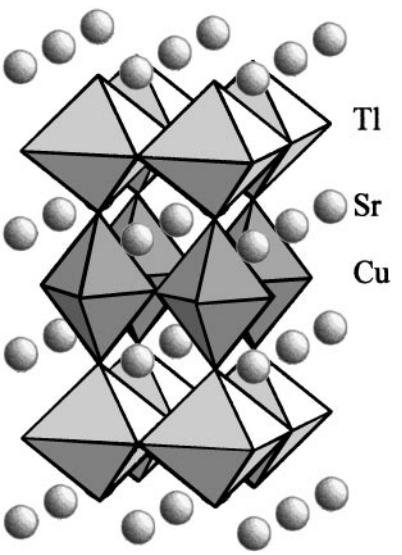

FIG. 2. Structure of the 1201 thallium cuprate $TlSr_2CuO_5$.

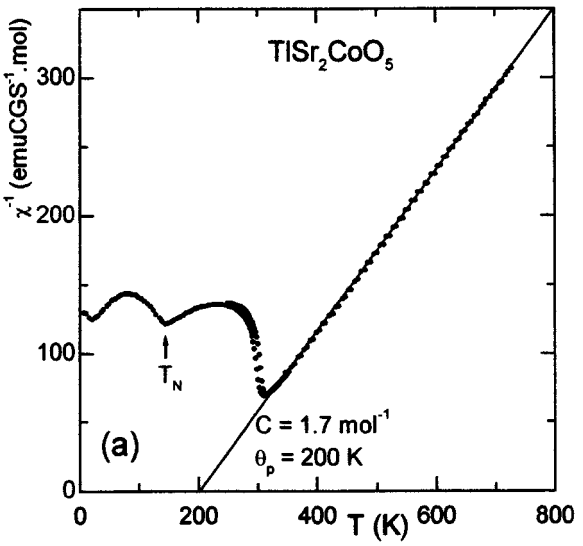

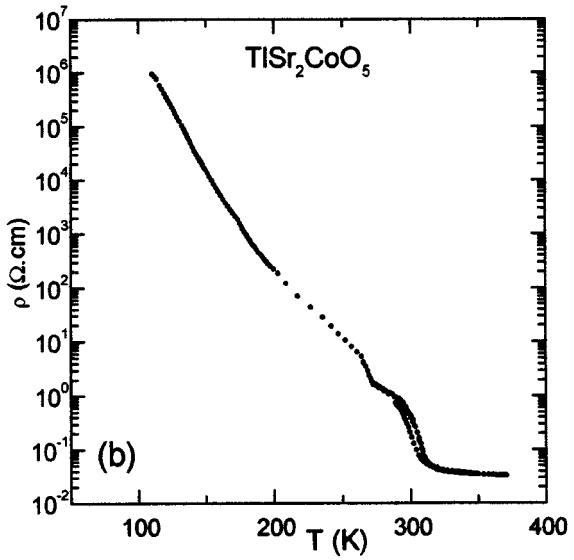

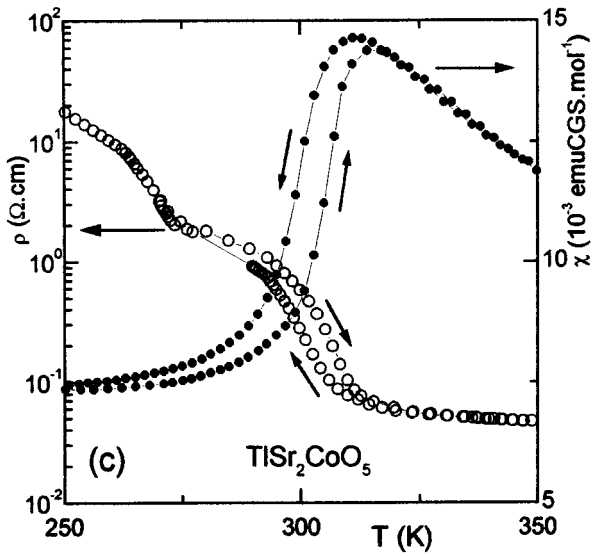

FIG. 3. Temperature dependencies of the magnetic susceptibility (a) and of the electrical resistivity (b) of $TlSr_2CoO_5$. Hysteresis effect around room temperature (c).

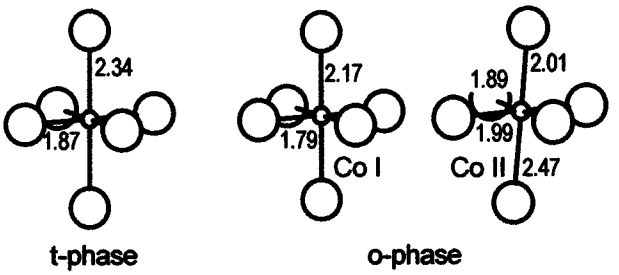

FIG. 4. Surrounding of the Co atoms in the *t*-phase and in the two sites of the *o*-phase.

Reflection conditions showed that the Bravais lattice is centered, two space groups being possible (*Cmcm* and $Cmc2_1$). A Rietveld refinement of high resolution X-ray synchrotron data using the most symmetrical space group (*Cmcm*) leads to two different sites for the Co atoms (5). A drawing of the Co–O layers is given in Fig. 5. Site I —occupied by one third of the cobalt atoms—is an elongated octahedron characterized by four very short equatorial Co–O distances of 1.79 A. Site II no longer has a D_{4h} point symmetry, one of the Co–O distances becoming very long (2.47 A) and thus leading rather to a 5-fold coordination (Fig. 4). The average Co–O distance is much shorter for site I (1.91 A) than for site II (2.04 A) the latter being very close to that in that *t*-phase (2.03 A).

4. BAND STRUCTURE CALCULATIONS

Band structure calculations were performed with the EHTB method (6–8). As the EHTB method uses the complete structural and chemical data (i.e., atomic orbitals and their overlap) it is well suited for the study of the interplay between electronic and crystal structures, in relation with chemical bonding features (9–12). It gives a quantitative information about quantities governed by the topology of interactions: hybridizations, band shape, Fermi surface, etc. However, it is not of the self-consistent field type and, for the study of energetic quantities such as band widths, band gaps, and crystal field parameter, it should be used only in a comparative strategy. This is the case in the present paper where the density of states (DOS) curves showing the contributions of the different *d* orbitals of the cobalt atoms were computed for the HT and LT phases of $TlSr_2CoO_5$ and compared.

The full crystal structures of $TlSr_2CoO_5$ at high and low temperatures were used for the computation. A 550 *k*-points grid was used to represent the irreducible wedge of the tetragonal Brillouin zone for the *t*-phase. For the LT

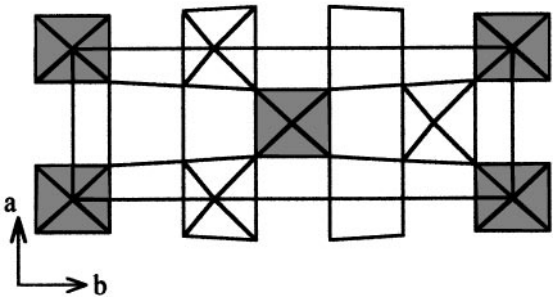

FIG. 5. Drawing of a CoO_2 layer in the *o*-phase. Site I is shown in gray.

structure, a 504 *k*-points grid was used for half a primitive unit cell of the reciprocal lattice. Extended Hückel parameters are given in Table 1. Calculations were performed on a CRAY-T3E computer, with a code adapted from the EHMACC program (No. 571 from the Quantum Chemistry Exchange Program).

In the *t*-phase Co^{3+} ions occupy a single type of site of D_{4h} symmetry. Projected DOS for cobalt 3*d*-orbitals are given in Fig. 6a. Bands originating from thallium 6*s* orbitals are found above -9 eV and those originating from oxygen 2p orbitals lie between -14 and -17 eV. As a result of the strong elongation of the CoO_6 octahedra the d_{z^2} band drops and overlaps the d_{xy}, $d_{xz,yz}$ ones. On the contrary the antibonding $\sigma^*_{x^2-y^2}$ band is lifted at a much higher energy as it involves the strongest overlaps between Co:3*d* and O:2*p* orbitals arising from the four short equatorial Co–O distances. Despite its narrowness it corresponds to itinerant electronic states with large effective mass. Such a result can be ascribed to the interactions of 3*d* orbitals of the metal with the 2*s* orbitals of oxygen that lead to a smaller dispersion, whereas the overlap increases, as already discussed by two of us (11).

TABLE 1
Extended Hückel Parameters: Energies and ζ Exponents of Slater-Type Atomic Orbitals

Element	Orbital	H_{ii} (eV)	$\zeta_i(c_i)$
Tl	6s	-11.60	2.30
	6p	-5.80	1.60
Sr	5s	-6.62	1.214
	5p	-3.92	1.214
Co	3d	-13.18	5.55 (0.5679)
			2.10 (0.6059)
	4s	-9.21	2.00
	4p	-5.29	2.000
O	2s	-32.30	2.275
	2p	-14.80	2.275

Note. Coefficients of double-ζ expansions are given in brackets.

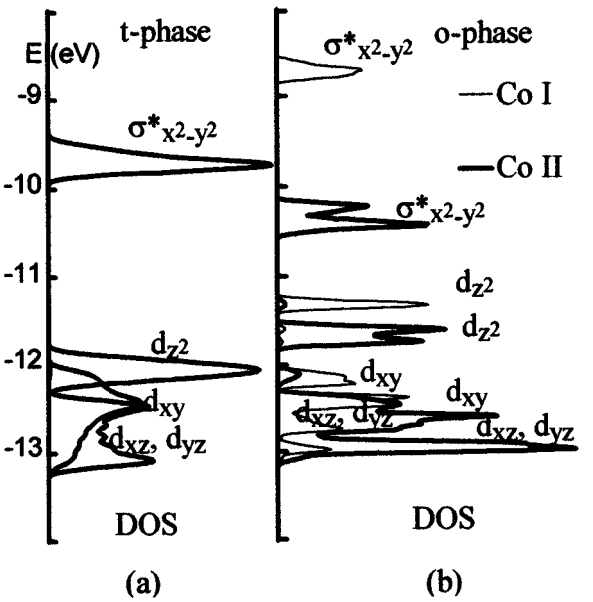

FIG. 6. Contributions of the 3*d* orbitals to the DOS for the *t*-phase (on the left-hand side) and for the *o*-phase (on the right-hand side where the thin line corresponds to site I and the bold line to site II).

In the LT phase two different surroundings are available for Co^{3+} ions (Fig. 4) and each of them leads to a band diagram reflecting the site environment as illustrated in Fig. 6b. The $\sigma^*_{x^2-y^2}$ band corresponding to site I is strongly shifted upwards by the very short Co–O equatorial distances. The splitting of most of the bands associated with site II accounts for the existence of two different apical distances. The bands are narrower for sites I that are isolated than for sites II that form zigzag chains.

The results of this EHTB calculation are further discussed and used for interpreting the physical properties of the investigated material in the following.

5. DISCUSSION

5.1. Magnetic Behavior

The magnetic susceptibility of the metallic *t*-phase follows a Curie–Weiss law $\chi = C/(T-\theta)$ characterized by a molar Curie constant $C = 1.7$ and a Weiss constant $\theta = +200$ K (Fig. 3). The latter denotes strong ferromagnetic interactions in the CoO_2 planes. We already have ascribed them to an indirect coupling of the *local* atomic spins *via* itinerant electrons. Whether the interaction is better described by the RKKY mechanism (13) or by the double-exchange mechanism introduced by Zener (14) for interpreting the ferromagnetic interaction in mixed valent manganites (parent compounds of the CMR materials) is out of the scope of the present paper. Nevertheless it should be emphasized that the double-exchange mechanism can be viewed as the

narrow-band limit (15) or as the low carrier-density limit (16) of the RKKY interaction.

In order to account for the experimental C-value of 1.7, Coutanceau *et al.* (4) assumed in a preliminary interpretation that all the Co^{3+} ions in the t-phase were in a high spin state, that the electrons located in a broad unsplit $\sigma^*_{x^2-y^2}$ band were itinerant, and that only the atomic *local* spin ($S = 3/2$) contributed to the temperature-dependent paramagnetism. In this model a spin-only value of C of 1.875 is expected (the 5% of cobalt (IV) atoms just leading to a lowering of the Fermi level in the $\sigma^*_{x^2-y^2}$ band), which is not very far from the experimental data. However, we now think that it is more correct considering that the *Hund's rule coupling* favors the polarization of the carrier spins in the $\sigma^*_{x^2-y^2}$ band and therefore that the itinerant electrons contribute to the Curie constant. Now the only way to account for the observed C-value is considering that each Co ion contribute for less than one electron, say x electron (with $x < 1$), to the conduction band, which implies that there are more than one electron with minority spin function in the localized d_{xz}, d_{yz} orbitals. This assumption may also be sketched as follows. If we call α the majority spin function and β the minority spin function the average electronic configuration of cobalt ions can be written as

$$(d_{xz}, d_{yz})^2_\alpha\ (d_{xz}, d_{yz})^{2-x}_\beta (d_{xy})^1_\alpha (d_{z^2})^1_\alpha\ (\sigma^*_{x^2-y^2})^x_\alpha.$$

A rigorous calculation of the theoretical value of the Curie constant of such a system, which by comparison with the experimental value would allow a determination of x, is not straightforward. However, as according to our EHTB calculations the $\sigma^*_{x^2-y^2}$ is rather narrow and as the itinerant-electron spins remain in some way coupled with the localized-electron spins we will assume that, in a first simple approach, a spin-only value of the Curie constant can be computed if we regard the system as a mixture of x atoms in a HS spin state with $(1 - x)$ atoms in an IS state. A similar procedure for the evaluation of the effective moment has been previously used for the metallic phase of $LaCoO_3$ (2). Finally, this leads to $x = 0.35$ (or 0.38 if we take into account the small deviation from stoichiometry of our sample, but the difference is not significant with respect to the crudeness of the approximations).

The magnetic behavior of the LT o-phase is complex. A kink at 150 K is due to the onset of a long-range spin ordering that has been evidenced by a Mössbauer study of a ^{57}Fe-doped sample (17). The susceptibility below 150 K decreases with decreasing temperature in a way more or less similar to that expected for an antiferromagnet.

The behavior above 150 K is more difficult to interpret. It was not possible to have a direct experimental determination of the spin states of Co^{3+}-ions by EPR. However most of the Co atoms must have an atomic spin differing from zero in order to account for the large magnetic susceptibility of the material and for the high magnetic-ordering temperature.

Let us first consider Co atoms in site II and compare their status with that of Co atoms in the t-phase. We note that the average Co–O distance is very close in both phases suggesting a crystal field parameter on the same order of magnitude. For site II equatorial Co–O distances are larger than in the t-phase. This suggests that for site II the $\sigma^*_{x^2-y^2}$ band should drop to a lower energy, which is confirmed by the EHTB calculation (Fig. 6). As the $\sigma^*_{x^2-y^2}$ band is partly occupied in the metallic phase we may conclude that Co^{3+} ions in site II of the insulating phase are in a HS state.

Which is the electronic configuration in site I? With four very short equatorial Co–O distances the $\sigma^*_{x^2-y^2}$ band is strongly shifted upward (Fig. 6) and therefore is very unlikely occupied. Thus in site I the electronic configuration could be either LS or IS, but we speculate that at 150 K the proportion of IS ions is already large in sites I for the following reason. Figure 5 shows that sites II form zigzag chains along the a-axis and the Co–O–Co superexchange interactions (with angles near 180°) involving half occupied $d_{x^2-y^2}$ orbitals should be antiferromagnetic (18). If sites I were occupied only by LS cations interchain coupling would be small even within the CoO_2 planes. We think that under such conditions one could hardly account for a 3D long-range ordering setting on at a Néel temperature as high as 150 K and therefore that a significant part of the sites I is occupied by IS ions.

We may further speculate about the magnetic ordering at low temperature. Site I–site II interactions involve an empty and a half-filled orbital $d_{x^2-y^2}$ that, according to the well known Goodenough–Kanamori rules, should be ferromagnetic. Thus we may see the long range ordering in the CoO_2 planes as antiferromagnetic double chains coupled ferromagnetically by site I Co atoms or alternatively ferromagnetic triple chains coupled antiferromagnetically. CoO_2 planes should be coupled antiferromagnetically to each other as the superexchange (*via* a O–Tl–O bonding) should mainly involve half-filled d_{z^2} orbitals for all the cation types.

As the temperature increases above 150 K one would have expected a decrease of the magnetic susceptibility following a Curie–Weiss law. On the contrary it does not, but it even tends to increase for temperatures above 240 K. Such a behavior can mainly come from the formation of increasing amounts of the HT phase which—even in small quantities—can significantly contribute to the magnetic susceptibility as it carries strong ferromagnetic interactions.

5.2. Electric Properties and the MI Transition

The metallic character of the HT t-phase is ascribed to a delocalization of the electrons in the $\sigma^*_{x^2-y^2}$ band of Co^{3+} ions. Using the temperature dependence of the Seebeck coefficient it is possible to show that this metallic behavior is

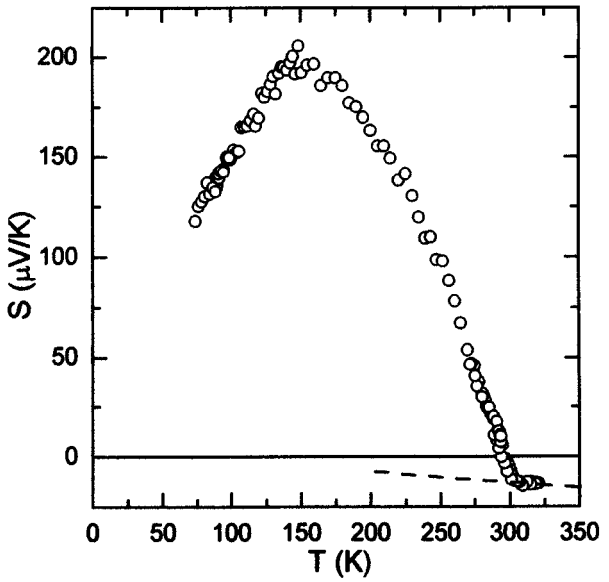

FIG. 7. Temperature dependence of the Seebeck coefficient of $TlSr_2CoO_5$ showing a change of sign at the MI transition.

not due to the thallium deficiency and its resulting hole formation as, for instance, in a degenerate semiconductor. Actually, the Seebeck coefficient is positive at low temperature, which reveals that carriers in the insulating phase are holes that we identify with Co^{4+} ions in agreement with the above description (Fig. 7). However near room temperature it changes sign showing that the HT form is a *n*-type metal and holes are no longer the predominant charge carriers. This result well agrees with our discussion of the magnetic properties that led to about 0.35 electron per atom in the σ band. It may also be pointed out that assuming all the cations are in a purely HS state encounters the following difficulty. A half-filled σ^* band should split into two Hubbard bands and the system should be a Mott–Hubbard (or a charge transfer) insulator that could become a *p*-type degenerate semiconductor upon doping and the Seebeck coefficient should be positive. On the contrary in our model only one sixth of the σ^* band is occupied and we predict a metallic HT-phase even for an ideally stoichiometric sample.

Then we depict the metallic phase as illustrated in Fig. 8. Roughly, about two third of the Co cations are in an IS state and one third in an HS state or, in order to account for the metallic character, we could regard the latter as IS Co^{4+} plus one *d*-electron in the σ^* conduction band. This electron may be the one that couples ferromagnetically the local moments, but, if so, it is not obvious that the interaction would be strong enough for giving rise to a Weiss constant as large as 200 K. Actually we may easily imagine that the ferromagnetic coupling is reinforced by the hopping of the fourth electron occupying the (d_{xz}, d_{yz}) orbitals onto a neighboring pseudo-HS cation. We emphasize that from a crystallographic point of view there is a single site for Co atoms in agreement with X-ray data, the fluctuations of the electronic states being dynamic in the same sense as, for instance, one speaks of dynamic Jahn–Teller effect if one considers intraatomic electron transfer or one speaks of polaron hopping if one considers interatomic charge transfer.

Upon decreasing temperature some vibration modes soften and as usually expected a static distortion takes place provided that it favors an electronic state of lower energy. We have already given above a detailed description of the LT phase. Comparing the two phases we may summarize the characteristics of the MI transition:

— it is a first order transition with a structural change,

— the density of the HT phase is larger than that of the LT phase. According to our picture this effect (that accounts for a strong electron–phonon coupling) mainly results from a decrease of the electron number in the σ^* antibonding levels and from an electronic delocalization, both contributing to decrease the cation–anion distance.

— it is associated with a change of the sign of the magnetic interactions as the LT phase is an antiferromagnetic insulator whereas the HT phase is a metal with dominant ferromagnetic interactions,

— the sign of the Seebeck voltage changes, denoting a transition from a *p*-type semiconductor to a *n*-type metal.

6. CONCLUSIONS

In the HT phase the electronic configuration of Co^{3+} ions can be regarded as intermediate between high-spin and intermediate-spin states. In the LT phase it disproportionates into a high-spin state for Co^{3+} ions in site II and an intermediated-spin state for Co^{3+} ions in site I. In some way

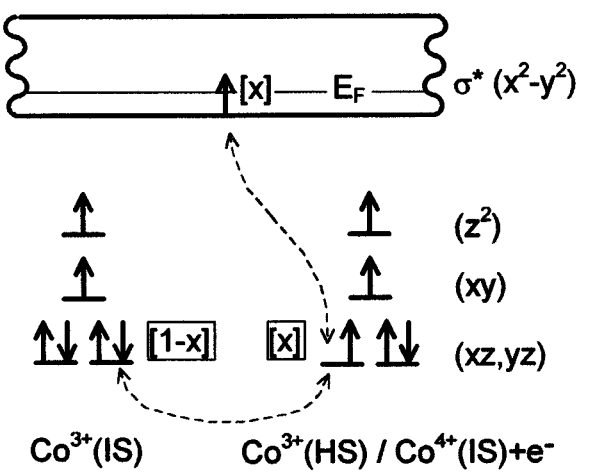

FIG. 8. Picturing the electron delocalization and the spin states in the metallic phase. Note the role that electrons in d_{xz}, d_{yz} orbitals could play for enhancing the ferromagnetic coupling.

the MI transition can be viewed as the analog of a Peierls transition in the sense that the stabilization of the electronic system is at the expense of the structural distortion. However here the situation is more complex as not only band states but also local electronic states play a major part in the process.

As a conclusion we would like to emphasize the relevance of the present compound and investigation to recent and important challenges for materials chemistry such as high T_c superconductors and CMR materials where most of the effects discussed here are present. So far as technological applications are concerned the first order MI transition occurring at room temperature could be of interest in the field of sensors or information storage.

REFERENCES

1. B. Buffat, G. Demazeau, M. Pouchard, and P. Hagenmuller, *Proc. Indian Acad. Sci.* **93,** 313 (1984).
2. M. Senaris-Rodriguez and J. B. Googenough, *J. Solid State Chem.* **116,** 224 (1995).
3. M. Coutanceau, J. P. Doumerc, J. C. Grenier, P. Maestro, M. Pouchard, and T. Seguelong, *C. R. Acad. Sci. Paris.* **320,** 675 (1995).
4. M. Coutanceau, J. P. Doumerc, J. C. Grenier, M. Pouchard, and D. Sedmidubsky, *Solid State Commun.* **96,** 569 (1995).
5. M. Coutanceau, A. Demourgues, J. C. Grenier, and J. P. Doumerc, To be published.
6. R. Hoffmann, *J. Chem. Phys.* **39,** 1397 (1963).
7. J. H. Ammeter, H. B. Bürgi, J. C. Thibeault, and R. Hoffmann, *J. Am. Chem. Soc.* **100,** 3686 (1978).
8. M. H. Whangbo and R. Hoffmann, *J. Am. Chem. Soc.* **100,** 6093 (1978).
9. J. K. Burdett and S. A. Gramsh, *Inorg. Chem.* **33,** 4309 (1978).
10. E. Canadell and M. H. Whangbo, *Chem. Rev.* **91,** 965 (1991).
11. A. Villesuzanne and M. Pouchard, *C. R. Acad. Sci. Paris* **310,** 155 (1996).
12. A. Simon, *Angew. Chem. Int. Ed. Engl.* **36,** 1788 (1997).
13. R. J. Elliott, "Magnetism" (G. T. Rado and H. Suhl, Eds.), Vol. IIA, p. 385. Academic Press, New York, 1965.
14. C. Zener, *Phys. Rev.* **82,** 403 (1951).
15. J. B. Goodenough, *Private communication.*
16. N. F. Mott, "Metal-Insulator Transitions," 2nd ed., p. 97. Taylor & Francis, London, 1990.
17. L. Fournes, A. Wattiaux, *Private communication.*
18. J. B. Goodenough, *Progr. Solid State Chem.* **5,** 145 (1971).